The N-terminal domain of the R28 protein promotes *emm28* group A *Streptococcus* adhesion to host cells via direct binding to three integrins

Received for publication, May 23, 2018, and in revised form, August 20, 2018 Published, Papers in Press, August 27, 2018, DOI 10.1074/jbc.RA118.004134

Antonin Weckel[‡§¶], Dorian Ahamada[‡§¶], Samuel Bellais[‡§¶1], Céline Méhats[‡§¶], Céline Plainvert[‡§¶‖], Magalie Longo[‡§¶], Claire Poyart[‡§¶‖**], and Agnès Fouet[‡§¶‖2]**

*From the [‡]INSERM U1016, Institut Cochin, [§]CNRS UMR 8104, and [¶]Université Paris Descartes, UMR-S1016 Paris, France and the [‖]Centre National de Référence des Streptocoques and the **Hôpitaux Universitaires Paris Centre, Institut Cochin, Assistance Publique Hôpitaux de Paris, 75014 Paris, France*

Edited by Chris Whitfield

Group A *Streptococcus* (GAS) is a human-specific pathogen responsible for a wide range of diseases, ranging from superficial to life-threatening invasive infections, including endometritis, and autoimmune sequelae. GAS strains express a vast repertoire of virulence factors that varies depending on the strain genotype, and many adhesin proteins that enable GAS to adhere to host cells are restricted to some genotypes. GAS *emm28* is the third most prevalent genotype in invasive infections in France and is associated with gyneco-obstetrical infections. *emm28* strains harbor R28, a cell wall–anchored surface protein that has previously been reported to promote adhesion to cervical epithelial cells. Here, using cellular and biochemical approaches, we sought to determine whether R28 supports adhesion also to other cells and to characterize its cognate receptor. We show that through its N-terminal domain, $R28_{Nt}$, R28 promotes bacterial adhesion to both endometrial– epithelial and endometrial–stromal cells. $R28_{Nt}$ was further subdivided into two domains, and we found that both are involved in cell binding. $R28_{Nt}$ and both subdomains interacted directly with the laminin-binding $\alpha3\beta1$, $\alpha6\beta1$, and $\alpha6\beta4$ integrins; interestingly, these bindings events did not require divalent cations. R28 is the first GAS adhesin reported to bind directly to integrins that are expressed in most epithelial cells. Finally, $R28_{Nt}$ also promoted binding to keratinocytes and pulmonary epithelial cells, suggesting that it may be involved in supporting the prevalence in invasive infections of the *emm28* genotype.

Streptococcus pyogenes, also known as group A *Streptococcus* (GAS),[3] is a Gram-positive bacterium responsible for a wide range of diseases, from superficial infections such as pharyngitis and dermatitis, to severe invasive infections such as necrotizing fasciitis and endometritis (1–3). GAS infections are also responsible for postinfectious complications such as rheumatic arthritis and glomerulonephritis, and altogether, GAS infections are responsible for 517,000 deaths annually worldwide (4).

GAS strains are genetically diverse and are genotyped through sequencing of the 5′ end of the *emm* gene (5) encoding the M protein, a major virulence factor; more than 250 *emm*-types have been described (6). A link exists between genotype and tissue tropism, with throat and skin specialists and ubiquitous genotypes (7); a link between genotype of invasive strains and elicited disease exists for some but not all genotypes.[4] Approximately 10% of the GAS genome is composed of exogenous genetic elements encoding virulence factors, with substantial variation between different *emm* types, which could account for the tropism (8). The first to third most prevalent genotype in Europe, *emm28*, is responsible for 8% of GAS invasive infections in France (9, 10, 34). It is associated with endometritis, and for example, in France, 27% of GAS invasive infections in women occur in the gyneco-obstetrical sphere (10–13). *emm28* strains harbor an integrative conjugative element named RD2 that was likely horizontally transferred from *Streptococcus agalactiae*, also known as group B *Streptococcus* (GBS) (13, 14). GBS colonizes 10–30% of healthy women's urogenital tract (15), and it was suggested that the presence of this integrative conjugative element accounts for the *emm28* GAS gyneco-obstetrical tropism (13). This remarkable tissue association together with the high prevalence of *emm*28 strain invasive infections prompted us to study the role of R28, an RD2 encoded surface protein, in GAS *emm*28 infections.

Adhesion to host tissues is the initial step for all GAS infections. It is mediated by different factors, mainly surface proteins, that bind either extracellular matrix components, indirectly to the cell surface through plasmatic or extracellular matrix components bridging or directly to eukaryotic receptors (reviewed in Refs. 16 and 17). RD2 encodes four surface proteins including R28, and a R28-deficient *emm28* strain is nonadherent to the cervical cell line ME180 (18). R28 is a

This work was supported by Paris Descartes University Contract KL2UD and Ecole Normale Supérieure, Paris, France (to A. W.) and funds from the Département Hospitalo–Universitaire Risks in Pregnancy 2014 (to A. F. and C. M.). The authors declare that they have no conflicts of interest with the contents of this article.
This article contains Tables S1 and S2, Figs. S1–S3, and a data file.

[1] Present address: Bioaster, 28 Rue du Dr. Roux, 75015 Paris, France.
[2] To whom correspondence should be addressed: Institut Cochin, 22 Rue Méchain, 75014 Paris, France. Tel.: 33-1-40-51-64-50; Fax: 33-1-40-51-64-54; E-mail: agnes.fouet@inserm.fr.

[3] The abbreviations used are: GAS, group A *Streptococcus*; GBS, group B *Streptococcus*; hDSC, human decidual stromal cell; ACP, αC protein; nt, nucleotide(s); ANOVA, analysis of variance; DAPI, 4′,6′-diamino-2-phenylindole; DSHB, developmental studies hybridoma bank; ERDF, European Regional Development Fund.

[4] C. Plainvert and C. Poyart, unpublished data.

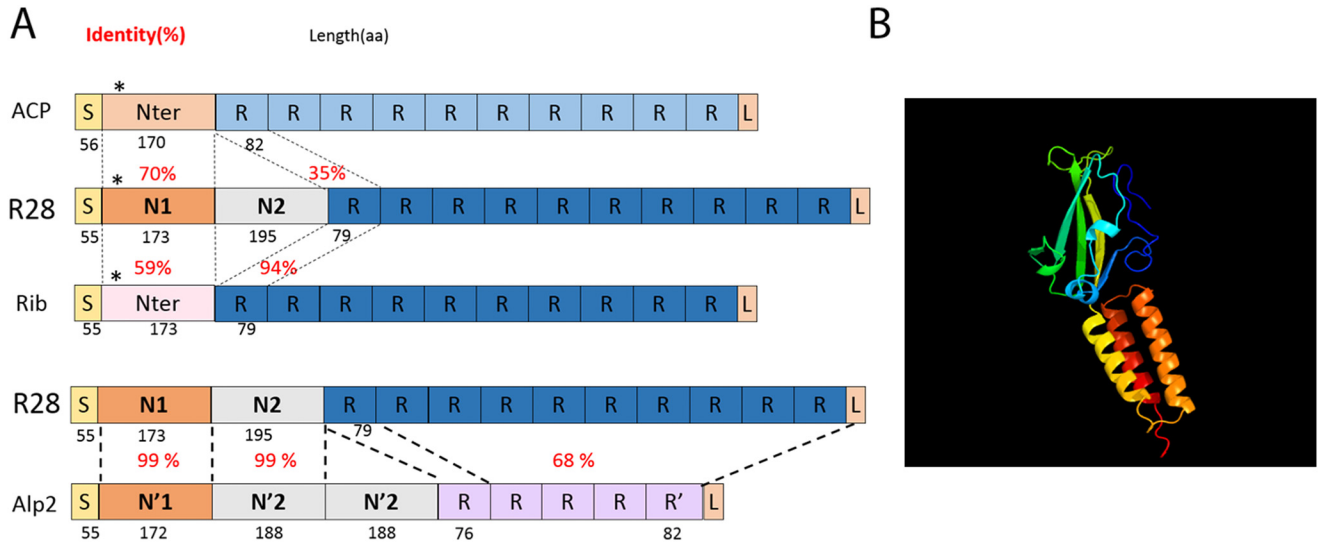

Figure 1. Schematic representation of R28, Alp family members, and R28-N1 predicted 3D structure. *A*, schematic representation of the Alp family members structure and similarity. *Numbers* in *black* below the scheme indicate the length in amino acid residues, and numbers in *red* indicate the percentages of identify between two domains. *S*, signal peptide; *R*, repeats; *L*, LP*X*TG. *, KTD in ACP, KAD in R28, and KPD in Rib. Modified with our sequence comparisons from Refs. 1–3. *B*, R28-N1 structure as predicted by Phyre. *Green* and *yellow*, the β-sandwich; *yellow* to *red*, the three-helix bundle.

member of the Alp family composed of GBS proteins that share evolutionary and structural similarity and which includes the αC protein (also known as ACP or α), Rib, R28 (also known as Alp3 in GBS), and Alp2 (18–21) (Fig. 1*A*). These chimeric proteins are composed of a signal peptide, an N-terminal domain, repeats, and an LP*X*TG anchoring motif. The repeat number varies among clinical isolates, and their structure is related to the Ig-like fold (22). The repeats are identical within one protein and the identity percentage between Alp members varies between 35 and 94, the latter being between Rib and R28 repeats. Repeats are considered to properly expose the N-terminal domain at the bacterial surface, potentially the functional domain (21). This domain is composed of one module for ACP and Rib, two modules for R28, and three modules for Alp2. The first modules of R28 and Alp2 share 99% identity and are 70 and 56% identical to the module of ACP and Rib, respectively. The second modules of R28 and Alp2 are 99% identical and is similar to the β protein, unrelated to the Alp family. Alp2 third module is a repeat of the second one (Fig. 1*A*) (21, 23, 24). Thus, R28 is a chimer of ACP and the β protein for its N-terminal domain and Rib for its repeats, and it immunologically cross-reacts with both proteins (19, 25). ACP is the most studied member of the Alp family, and the crystal structure of the N-terminal domain has been elucidated (24). It binds glycosaminoglycans in a region encompassing the end of the N-terminal domain and the repeats (26, 27), and the α1β1 integrin through a KTD motif localized in a β-sandwich subdomain at the N-terminal end of its N-terminal domain (24, 28, 29); this motif is absent from R28, Alp2, and Rib (Fig. 1*A*). These interactions increase GBS internalization in the cervical cell line ME180 (29).

In this study, we analyzed the capacity of R28 to promote adhesion to host cells and characterized the adhesion domain. We demonstrate that the N-terminal domain of R28 (R28$_{Nt}$) is sufficient to promote direct adhesion to different gyneco-obstetrical cell lines and further identified two subdomains within R28$_{Nt}$ that are both involved in this adhesion process. We then characterized the chemical nature of the R28$_{Nt}$ receptor and isolated different ligands. We show that R28$_{Nt}$ interacts with the laminin-binding integrins α3β1, α6β1, and α6β4. Finally, we show that R28$_{Nt}$ increases adhesion also to skin and pulmonary cells, further extending the role of R28 as a GAS adhesin involved in GAS *emm28* prevalence.

Results

The N-terminal domain of R28 is sufficient to promote adhesion to human female genital tract cells

Association of GAS *emm28* strains with gyneco-obstetrical infections could be a consequence of its capacity to colonize the vaginal tract (10). A GAS R28-deleted mutant adheres less than the parental strain to cells from the cervical ME180 lineage (18). To assay the role of R28 in a more physiological situation, we tested whether the phenotype could also be observed on human decidual stromal cells (hDSCs) isolated from decidual biopsy of specimens obtained after caesarian delivery (Fig. 2*A*). The decidua is the lining of the uterine during pregnancy and consists of differentiated endometrial stromal fibroblasts and recruited leukocytes. It may be a direct target of GAS infection, a major cause of severe puerperal sepsis. The R28-deleted strain adhered significantly less (18%) to hDSCs than the WT strain (Fig. 2*A*), confirming the role of R28 as an adhesin on physiologically relevant cells. We then sought to characterize the adhesion domain of the R28 protein using different cells from the female genital tract, hDSCs as well as two cell lineages, cervical cells (ME180), often used to study female genital tract infections, and endometrial epithelial cells (HEC-1-A). The 6–17 highly conserved 79-residue-long repeats of R28 are considered to expose the 368-residue-long N-terminal domain at the bacterial surface, potentially the functional domain (Fig. 1*A*) (18, 29). Consequently, to analyze the ability of R28 to promote adhesion to various cells, we focused on the N-terminal

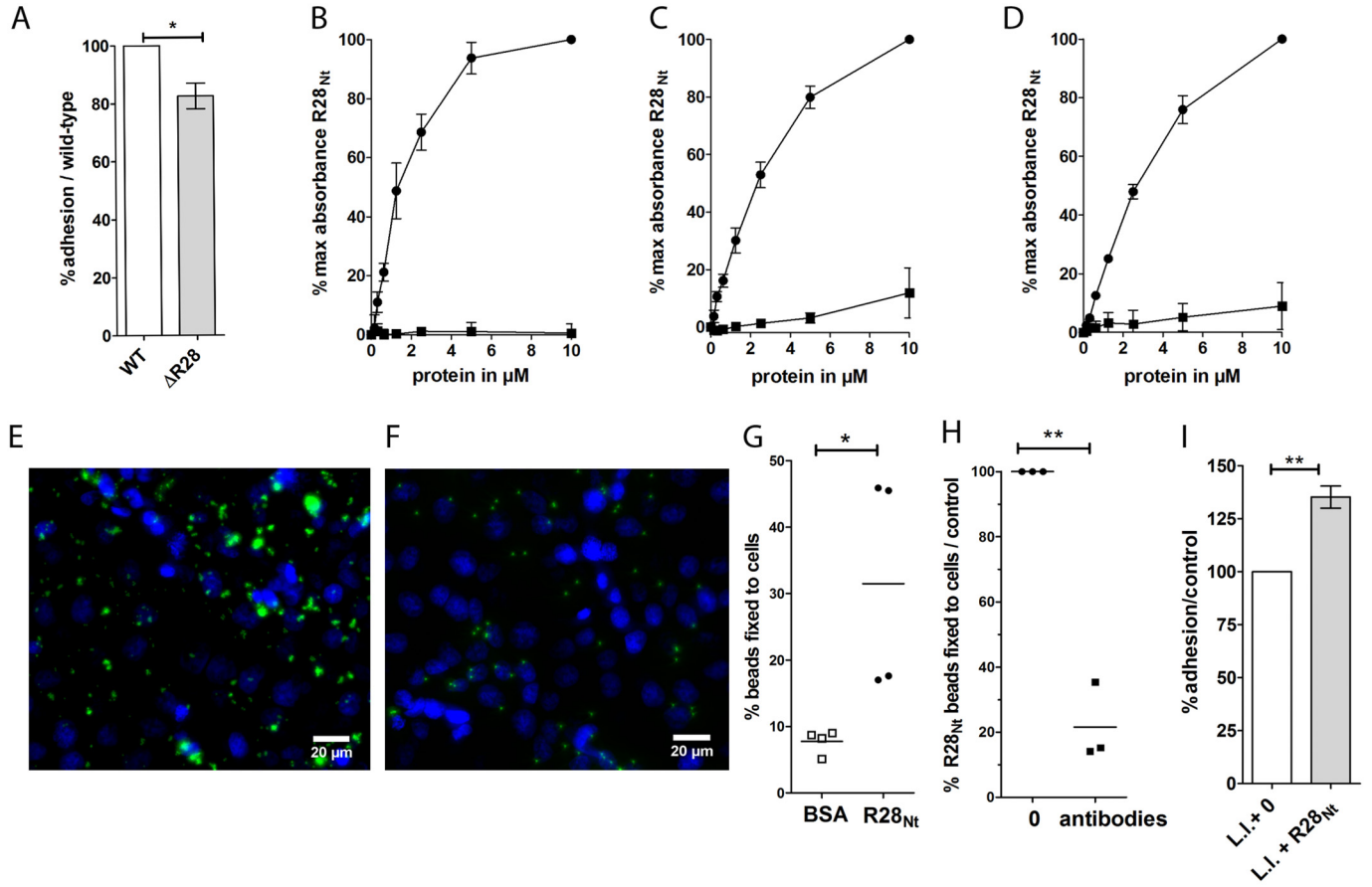

Figure 2. R28$_{Nt}$ is sufficient to promote adhesion to female genital tract cells. *A*, binding of the ΔR28 strain to hDSCs is expressed as a percentage of that of the WT strain; two-tailed *t* test was performed on six independent experiments performed in triplicate. *B–D*, ELISA-based protein–cell interaction assay with biotinylated proteins, expressed as percentages of the maximum binding, on secondary decidual cells (*B*), ME180 cells (*C*), and HEC-1-A cells (*D*). *Circles*, biotinylated R28$_{Nt}$; *squares*, biotinylated BSA. *Error bars* correspond to S.E. of four independent experiments. *E* and *F* representative immunofluorescence of coated fluorescent beads with R28$_{Nt}$ (*E*) or BSA (*F*) on HEC-1-A cells. Coated beads are in *green*, and DAPI staining is in *blue*. *G*, binding of R28$_{Nt}$ or BSA-coated fluorescent beads to HEC-1-A cells (one-tailed *t* test). *H*, binding of R28$_{Nt}$-coated fluorescent beads to HEC-1-A cells in the presence of purified anti-R28$_{Nt}$ antibodies, expressed as the percentage of that in the absence of anti-R28$_{Nt}$ antibodies. *I*, adhesion of R28$_{Nt}$ expressing *L. lactis* (L.l. + R28$_{Nt}$) to HEC-1-A cells, expressed as the percentage of that of the *L. lactis* empty vector strain (L.l. + 0). *H* and *I*, two-tailed *t* test. *, $p < 0.05$; **, $p < 0.01$.

domain of R28, R28$_{Nt}$, using biotinylated R28$_{Nt}$ (Fig. 2, *B–D*). R28$_{Nt}$ displays higher binding capacity to hDSC, ME180, and HEC-1-A cells than soluble BSA (200, 10, and 10 times more binding at 10 μM, respectively).

To confirm the capacity of R28$_{Nt}$ to promote adhesion, we tested whether R28$_{Nt}$-coated beads or a heterologous bacterium expressing R28$_{Nt}$ could bind more to HEC-1-A cells than the controls (Fig. 2, *E–I*). R28$_{Nt}$-coated beads adhered three times more than the BSA-coated control beads ($p < 0.05$) (Fig. 2, *E–G*), and this binding was blocked by the addition of purified R28$_{Nt}$ antibodies ($p < 0.05$) (Fig. 2*H*). Also, the *Lactococcus lactis* strain expressing R28$_{Nt}$ (Fig. S1*A*) adhered significantly more than the control strain harboring the empty vector (+35%, $p = 0.0066$) (Fig. 2*H*). The increased adherence may seem weak. However, in the absence of the repeats, R28$_{Nt}$ may be poorly exposed at the *L. lactis* cell surface or hidden by the protective polysaccharide pellicle (30) compared with the exposition of the complete R28 protein in GAS *emm*28 strains; this could lead to an underestimation of R28$_{Nt}$ capacity to promote adhesion. Thus, the N-terminal domain of R28 is sufficient to increase the adherence of a Gram-positive bacterium to endometrial cells. Altogether, these results demonstrate that R28$_{Nt}$ promotes bacterial adhesion to female genital tract cells.

Both N-terminal subdomains R28-N1 and R28-N2 are sufficient to promote adhesion to HEC-1-A cells

The R28$_{Nt}$ domain is composed of two halves: amino acid residues 56–229 and residues 230–424, which we termed R28-N1 and R28-N2, respectively (Fig. 1*A* and Fig. S1*B* (21). A BLAST alignment indicated that R28-N1 and R28-N2 share no similarity (E-value, 0.27). To test which subdomain mediates adhesion, we produced and purified the corresponding peptides (Fig. S1, *B* and *C*) and incubated them after biotinylation with ME180 and HEC-1-A cells (Fig. 3, *A–C*). Both the R28-N1 and R28-N2 subdomains showed significant binding with both cell types compared with BSA ($p < 0.001$ for both cell types), with R28-N2 displaying an affinity 2–3-fold higher than that of R28-N1 (Fig. 3*C*). The R28-N1 and R28-N2 binding values indicate an additive contribution of R28-N1 and R28-N2 to the R28$_{Nt}$ binding on HEC-1-A cells and a synergetic one on ME180 cells (Fig. 3*C*).

To assess the binding of these subdomains in more physiological conditions, we tested whether R28-N1– and R28-N2–

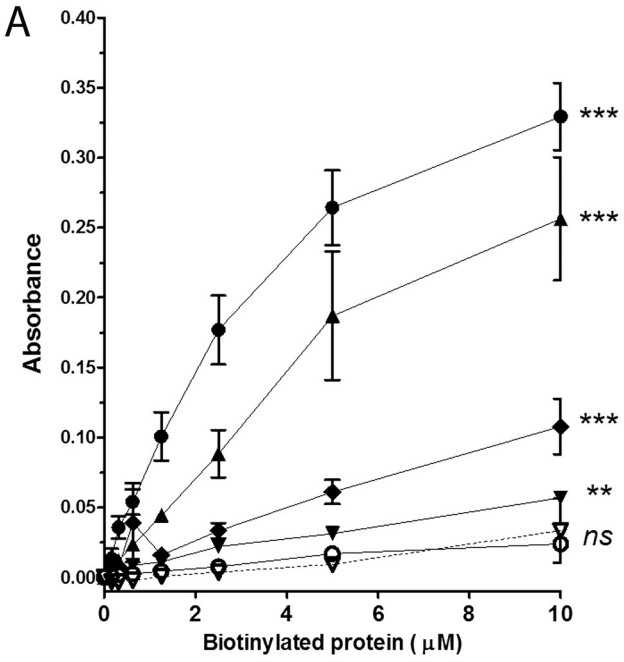

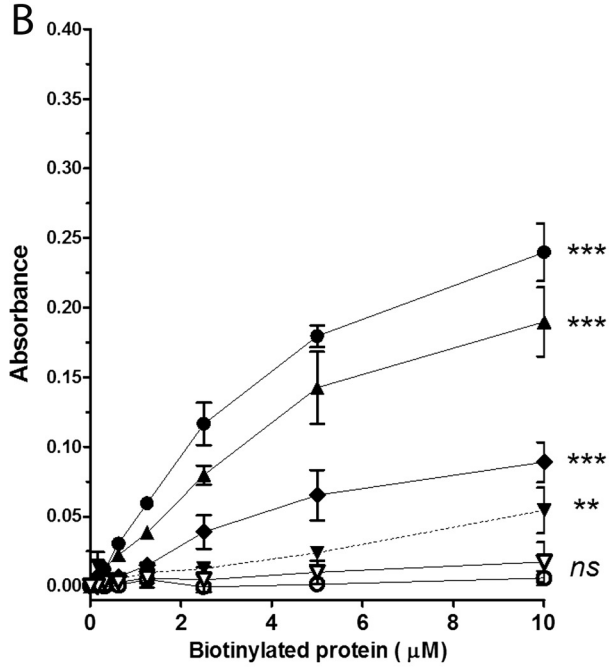

C

Cell type	HEC-1-A		ME180	
	B1	B2	B1	B2
R28-N1	0.0166	-0.0008	0.0156	-0.0005
R28-N2	0.0368	-0.0018	0.0440	-0.0018
R28$_{Nt}$	0.501	-0.0026	0.079	-0.0046
ACP$_{Nt}$	0.0038	-0.00002	0.0083	-0.0003

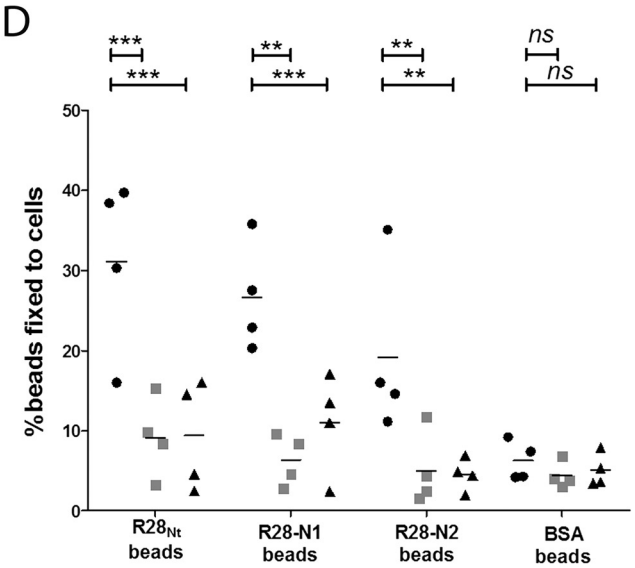

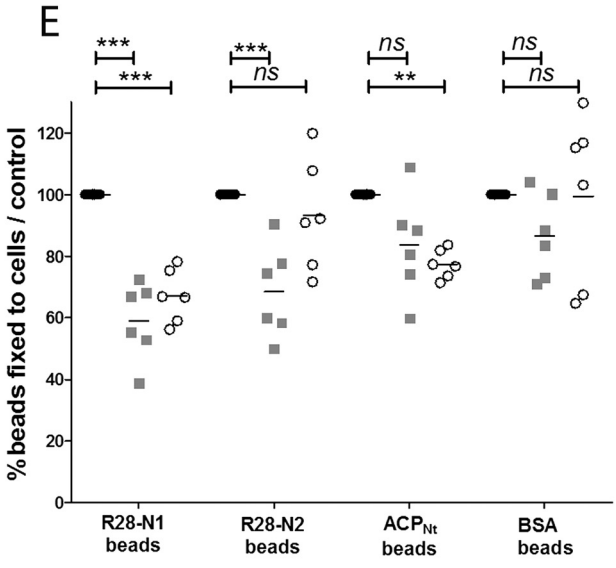

Figure 3. R28-N1 and R28-N2 subdomains and ACP$_{Nt}$ are sufficient to promote adhesion to HEC-1-A cells and compete differentially with each other binding. *A* and *B*, ELISA-based cell interaction assay with purified biotinylated R28$_{Nt}$ (●), the subdomains R28-N1 (◆) and R28-N2 (▲), ACP$_{Nt}$ (▼), Rib$_{Nt+2R}$ (○), and BSA (▽). Peptide solutions were incubated with ME180 cells (*A*) or HEC-1-A cells (*B*), washed, and fixed with paraformaldehyde, and bound biotinylated proteins were detected as in an ELISA. The experimental data for biotinylated R28$_{Nt}$ and BSA are those used for Fig. 2*C* and 2*D*. The calculation for the absorbance is described under "Experimental procedures." *Error bars* correspond to S.E. of four independent experiments performed in duplicate. *C*, parameters of the nonlinear fitting of figures *A* and *B*. *D* and *E*, fluorescent R28$_{Nt}$-coated (*D*), R28-N1– coated (*D* and *E*), R28-N2-coated (*D* and *E*), ACP$_{Nt}$-coated (*E*), or BSA-coated (*D* and *E*) beads were incubated with HEC-1-A cells preincubated with 20 μM of recombinant R28-N1 (■), R28-N2 (▲), or ACP$_{Nt}$ (○) or not preincubated (●). **, $p < 0.005$; ***, $p < 0.001$; *ns*, not significant.

coated beads bound HEC-1-A cells (Fig. 3*D*). Twenty-seven % and 19% of R28-N1– and R28-N2–coated beads bound to HEC-1-A cells, respectively, a percentage significantly higher than BSA-coated beads (6.3%, $p < 0.001$ and $p < 0.05$ for R28-N1 and R28-N2 with HEC-1-A cells, respectively). We checked the binding specificity of the coated beads by incubating cells with an excess amount of soluble peptides (20 μM) and assessing the percentage of beads still bound to cells (Fig. 3*D*). Purified R28-N1 and R28-N2 peptides competed with their respective coated beads (6.3 and 4.5% *versus* 27 and 19%, for R28-N1 and R28-N2, respectively), confirming the binding specificity. Altogether, these data clearly indicate that both the R28-N1 and R28-N2 subdomains are sufficient to promote adhesion to HEC-1-A cells.

We then sought to determine whether R28-N1 and R28-N2 have independent receptors. We performed competition assays in which we assessed the percentages of R28-N1– and R28-N2–coated beads bound to cells preincubated with excess amounts (20 μM) of soluble R28-N2 and R28-N1, respectively (Fig. 3*D*). These subdomains compete with one another ($p < 0.005$), suggesting that these subdomains share common receptor(s). Moreover, both displaced R28$_{Nt}$-coated beads, lowering its binding level to unspecific binding level (BSA-coated beads, 6%), further supporting that R28-N1 and R28-N2 share a common receptor.

R28$_{Nt}$ adhesive properties are not conserved among all Alp family members

Among members of the Alp family, ACP binds, through its N-terminal domain, the $\alpha1\beta1$ integrin (28) and, through a region encompassing the end of the N-terminal domain and the repeats, glycosaminoglycans (26, 27). In contrast, attempts to demonstrate that Rib is an adhesin have been unsuccessful (31). We focused on the shared N-terminal domains of these proteins, leaving out from ACP$_{Nt}$ the region binding glycosaminoglycans. A BLAST alignment indicated that R28-N1 is 70 and 56% identical to the N-terminal domains of ACP and Rib, respectively (Fig. 1*A*). Furthermore, a Phyre analysis predicted, with a confidence of 100%, that R28-N1 has the same structure as ACP, that is two domains, an N-terminal β-sandwich, sharing structural elements with the type III fibronectin fold and a C-terminal three-helix bundle (Fig. 1*B*) (24). We thus wondered whether the adhesive properties of R28-N1 to cervical and endometrial cells are conserved among the ACP or Rib N-terminal domains. We tested the binding capacity of ACP$_{Nt}$ and Rib$_{Nt+2R}$, which contains, in addition to the N-terminal domain, two repeats that are 94% identity to the R28 repeats (Fig. 1*A*). We expressed and purified these peptides and analyzed their direct binding to ME180 and HEC-1-A cells (Fig. S1, *C* and *D*, and Fig. 3, *A* and *B*). ACP$_{Nt}$ binds to both cell types, yet less than R28-N1 and consequently even less than R28-N2 or R28$_{Nt}$. Because ACP$_{Nt}$ binds HEC-1-A, despite the absence of $\alpha1\beta1$ integrin on its surface (32), we tested whether it shared a receptor with R28-N1 or R28-N2 by assaying, as for the R28-N1 and R28-N2 competitions, whether it can compete with R28-N1 and R28-N2 (Fig. 3, *D* and *E*). ACP$_{Nt}$ competes with itself and R28-N1 ($p < 0.005$), suggesting that these subdomains share a common receptor, but not with R28-N2 (Fig. 3*B*). Moreover, we did not detect a competition between R28-N1 and ACP-bound beads (Fig. 3*E*). In contrast to ACP, Rib$_{Nt+2R}$ does not bind to either ME180 or HEC-1-A cells, which indicates that this binding property is restricted to some Alp family members (Fig. 3, *A* and *B*). Moreover, because Rib$_{Nt+2R}$ contains two R28-like repeats, its inability to bind ME180 and HEC-1-A cells suggests that R28 repeats do not mediate the adhesion on their own.

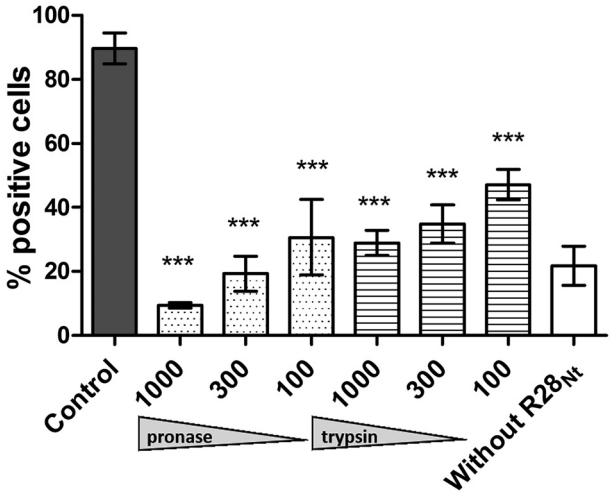

Figure 4. The R28$_{Nt}$ receptor is a cell surface protein. Analysis of the chemical nature of the R28$_{Nt}$ receptor was performed. Treatments were applied to HEC-1-A cells in suspension prior to incubation with purified R28$_{Nt}$; bound R28$_{Nt}$ is immunostained, and cells were analyzed by flow cytometry. *Dark column*, untreated cells; *white column*, unspecific labeling of cells without incubation of peptide. Statistical analysis was performed against the untreated condition. *Error bars* correspond to S.E. of three independent experiments (two-way ANOVA). ***, $p < 0.001$.

R28$_{Nt}$ receptor is a membrane protein

Our experiments were carried out in the absence of added extracellular or plasmatic protein; we consequently hypothesized that R28$_{Nt}$ binds directly to a cell surface receptor(s). To identify it, we first defined its chemical nature. As previously described (33), we applied to HEC-1-A cells different treatments that affect potential receptors depending on their chemical nature before incubating them with soluble R28$_{Nt}$ and quantifying bound R28$_{Nt}$ by flow cytometry (Fig. 4). Pronase and trypsin treatments significantly reduced, in a dose-dependent manner, the percentage of positively labeled cells down to 10 and 29%, respectively. Also, neither heparinase I nor sodium periodate treatments affected R28$_{Nt}$ binding to cells (data not shown), excluding an interaction between R28$_{Nt}$ and glycosaminoglycans or carbohydrates, which harbor vicinal hydroxyl groups. These results suggest that the R28$_{Nt}$ receptor is a cell surface–exposed protein. Similar results were obtained with R28-N1 and R28-N2 (Fig. S2, *A* and *B*). Altogether, our data suggest that the R28$_{Nt}$, R28-N1, and R28-N2 receptor(s) are a cell surface–exposed protein(s).

Identification of several putative receptors of R28$_{Nt}$

To identify R28 receptor(s), a co-immunoprecipitation experiment using HEC-1-A cells was set up followed by MS analysis. Cross-linked R28$_{Nt}$–cellular proteins complexes were resolved on acrylamide gels, and Western blotting highlighted

Table 1
Main hits from mass spectrometry analysis of specifically co-immunoprecipitated $R28_{Nt}$ receptors
A, absent from control conditions.

Common name	Gene name	Relative raw intensity		
		Experiment 1	Experiment 2	Experiment 3
Basal cell adhesion molecule	*BCAM*	A	3.50	5.00
Cadherin-1	*CDH1*	A	A	A
CD166 antigen	*ALCAM*	A	3.70	8.30
Desmoglein-2	*DSG2*	A	A	6.01
Ephrin type-A receptor 2	*EPHA2*	A	4.03	3.20
Integrin α3	*ITGA3*	A	8.32	65.32
Integrin α6	*ITGA6*	A	18.37	A
Integrin αV	*ITGAV*	A	1.74	7.20
Integrin β1	*ITGB1*	A	3.50	6.55
Integrin β4	*ITGB4*	A	5.84	5.62
Prostaglandin F2 receptor negative regulator	*PTGFRN*	A	A	A
Transferrin receptor protein 1	*TFRC*	A	3.54	5.10

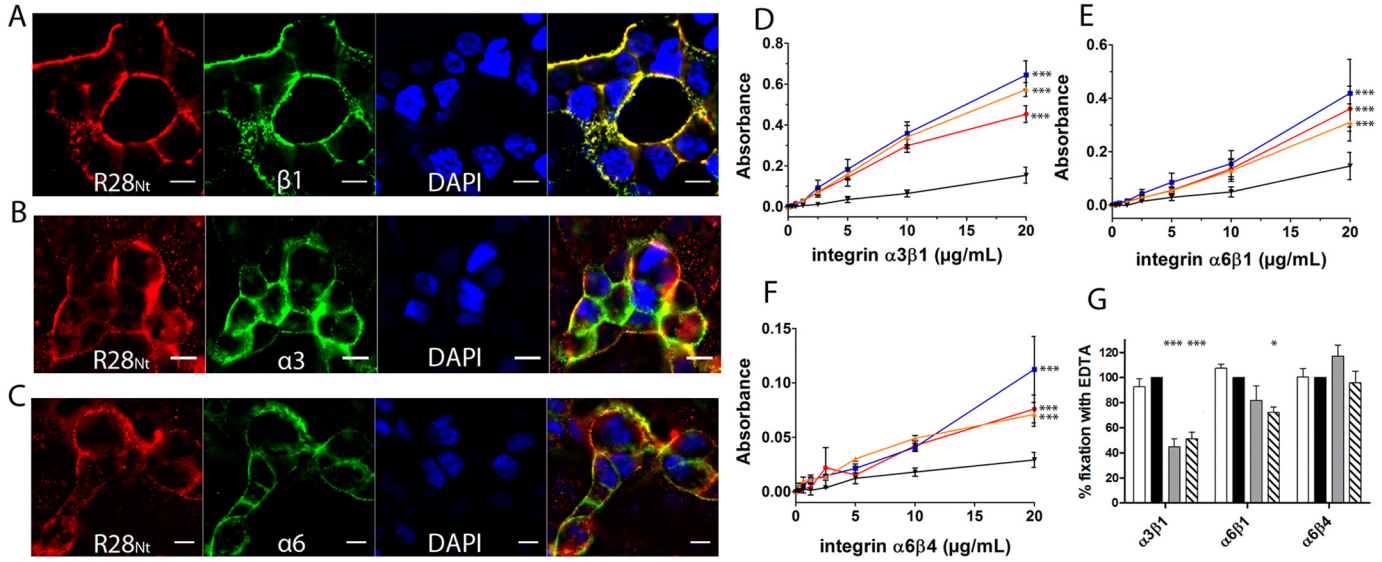

Figure 5. $R28_{Nt}$ and its subdomains interact with integrins α3β1, α6β1, and α6β4. *A–C*, immunostaining of $R28_{Nt}$ and different integrin monomers on HEC-1-A cells: β1 (*A*), α3 (*B*), and α6 (*C*). *Red*, $R28_{Nt}$; *green*, the specified integrin monomer; *blue*, DAPI; *far-right image*, merge. *Scale bars* correspond to 5 μm. *D–F*, assessment of integrin binding: α3β1 (*D*), α6β1 (*E*), and α6β4 (*F*) binding to $R28_{Nt}$ (*red*), R28-N1 (*blue*), R28-N2 (*orange*), or BSA (*black*) by ELISA. *Error bars* correspond to S.E. of three to five independent experiments (two-way ANOVA at 20 μg/ml with Bonferroni post-tests against BSA). *G*, role of divalent cations in the binding of integrins to $R28_{Nt}$, PBS (*white column*); PBS + EDTA (*black column*); PBS + Mn^{2+} (*gray column*); and PBS + Ca^{2+} (*hatched column*) (one-way ANOVA of four independent experiments). *, $p < 0.05$; ***, $p < 0.001$.

multiple high-molecular-mass (>170 kDa) complexes (data not shown) absent in the co-immunoprecipitation without $R28_{Nt}$ incubation (control). The zones above 170 kDa of $R28_{Nt}$ and control immunoprecipitations were excised from gels, and the protein contents were analyzed by MS (supporting data file). Hits enriched in the co-immunoprecipitation in the presence of the bait $R28_{Nt}$ in all three independent experiments were initially selected. From this list, and because the $R28_{Nt}$ receptors are cell surface– exposed proteins (Fig. 4), only such proteins were further selected (Table 1). Hence, through co-immunoprecipitation of $R28_{Nt}$, we identified several potential $R28_{Nt}$ receptors.

$R28_{Nt}$, R28-N1, and R28-N2 interact directly with integrins

Of all the proteins identified as present in the complexes co-immunoprecipitated with $R28_{Nt}$, we decided to focus on integrins as possible $R28_{Nt}$ receptors. To test this, we assayed by immunofluorescence whether soluble $R28_{Nt}$ and highlighted integrin monomers are in close proximity at the surface of HEC-1-A cells (Fig. 5, *A–C*). At the cell surface, $R28_{Nt}$ indeed binds into clusters in close proximity to integrin α3, α6, and β1 clusters.

To confirm a direct interaction between $R28_{Nt}$ and integrins, we analyzed the binding of the extracellular domains of integrins to $R28_{Nt}$, R28-N1, and R28-N2 by ELISA (Fig. 5, *D–F*). Integrins α3β1, α6β1, and α6β4 all interact significantly more with $R28_{Nt}$, R28-N1, and R28-N2 than with BSA ($p < 0.001$). To assess the binding specificity further, the same experiment was carried out with an integrin containing a subunit that, although it is expressed by HEC-1-A cells, had not been found in the MS analysis, namely α2β1 (Fig. S3) (32). In contrast to a natural ligand, type I collagen, neither $R28_{Nt}$ nor its two subdomains, R28-N1 and R28-N2, displayed interaction with α2β1, indicating that the integrins α3β1, α6β1, and α6β4 are true receptors of $R28_{Nt}$. The influence of divalent cations on the binding efficiency was assessed. As expected, binding of $R28_{Nt}$ to the different integrins in the presence of EDTA reflects that in PBS (Fig. 5*G*). Addition of the divalent ions Ca^{2+} significantly lowers binding of $R28_{Nt}$ to α3β1 and α6β1 (51 and 72% compared with in the presence of EDTA, respectively) and that of Mn^{2+} to

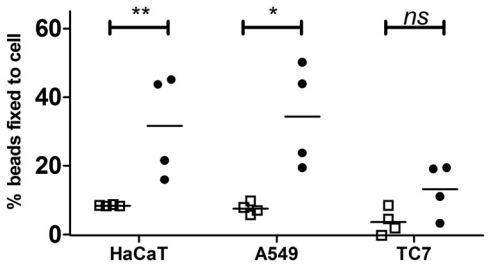

Figure 6. R28$_{Nt}$ increases binding to different cell lines. The figure shows binding of R28$_{Nt}$-coated (*black circles*) or BSA-coated (*empty squares*) fluorescent beads to different epithelial cell types: HaCaT (keratinocytes), A549 (pulmonary), and TC7 (intestine). Four independent experiments performed in duplicate (two-way ANOVA). *, $p < 0.05$; **, $p < 0.005$; *ns*, not significant.

$\alpha3\beta1$ (45%). In contrast, binding to $\alpha6\beta4$ was unchanged by the addition of divalent cations. Altogether, these data demonstrate the direct interaction between R28$_{Nt}$, R28-N1, and R28-N2 and the three integrins $\alpha3\beta1$, $\alpha6\beta1$, and $\alpha6\beta4$.

R28$_{Nt}$ is sufficient to promote adhesion to different cell lines

So far, our study focused on the capacity of R28 to promote adhesion to endometritis-related cells; yet *emm28* is the first to third most prevalent genotype for GAS invasive infections in Europe (9, 10). Moreover, the R28-interacting integrins are expressed by numerous cell types, so we assayed whether R28 contributes to adhesion in other GAS-elicited invasive infections. We tested R28$_{Nt}$ ability to promote adhesion to other cell lines by testing the binding capacity of R28$_{Nt}$-coated beads to skin keratinocytes, HaCaT, pulmonary epithelial cell, A549, as well as the gut intestinal cells TC7, that do not display the integrins $\alpha3\beta1$, $\alpha6\beta1$, and $\alpha6\beta4$ apically (Fig. 6) (35). R28$_{Nt}$-coated beads bind significantly and to a similar level (~30%) A549, HaCaT, and HEC-1-A cells (Figs. 2*G* and 6). In contrast, only 13% of R28$_{Nt}$-coated beads bind TC7 cells, not significantly different from the BSA-coated control beads. In conclusion, R28$_{Nt}$ is sufficient to promote adhesion to cell lines relevant not only for GAS endometritis but also for other GAS invasive infections.

Discussion

R28, a surface protein specifically expressed by *emm28* strains, which are associated with endometritis, promotes adhesion to cervical cells; its eukaryotic ligand was unknown (18). Currently in France, 50% of cases of GAS-elicited endometritis are associated with puerperal fever, abortion, *in vitro* fertilization, or spontaneous abortion,[4] all situations where stromal decidual cells line the endometrium. Thus, GAS elicited endometritis may be favored by GAS adhering to decidual cells, in addition to epithelial cervical or endometrial cells. The R28-deleted strain was hampered in its capacity to adhere to hDSCs (Fig. 2). That the mutant strain still adheres can be explained by the number of adhesins displayed by GAS strains (36–38), the deletion of a single one being insufficient for a total loss of adhesion capacity, as shown for example for Epf (39) and C5a peptidase (40). R28$_{Nt}$ binds to hDSCs, endometrial epithelial cells, and cervical epithelial cells; it also promotes the adhesion of beads or heterologous bacteria to endometrial epithelial cells (Fig. 2). These data altogether confirm the role of R28 as an adhesin and extends its role to other cells potentially involved during endometritis.

R28 belongs to the Alp family of proteins, shared with GBS, which includes ACP, Rib, and Alp2. The ACP N-terminal domain, but not that of Rib, also bound endometrial and cervical epithelial cells, indicating that this property is not limited to R28 but not shared by all the members of the Alp family either (Fig. 3). It is noteworthy that the ACP N-terminal domain shows a higher sequence identity to R28 N-terminal sequence than does Rib N-terminal domain, as well as a structural identity (18, 24); this could account for ACP but not Rib sharing the binding property. Furthermore, R28$_{Nt}$ and Alp2 N-terminal domain are nearly identical (20, 21); consequently this binding property could be extended to Alp2. The vaginal tracts of 15–30% of women are colonized by GBS, and all GBS strains present the gene encoding for one member of the Alp family (15, 41); most of these proteins are likely involved in GBS colonization.

The GBS proteins ACP and Alp3 (*i.e.* R28) bind glycosaminoglycan (26). Analysis using a set of constructions with different ACP domains suggested that a site beginning in the N-terminal region of ACP and extending into the repeat region is responsible for this binding (26, 27). Here, the R28$_{Nt}$ and ACP$_{Nt}$ peptides we used were devoid of repeat region sequences, suggesting that the binding we observed was not that to glycosaminoglycan; this was confirmed by the absence of heparinase treatment effect on the R28$_{Nt}$–HEC-1-A binding. This suggested that other receptors than glycosaminoglycan are involved in the R28-endometrial or -cervical cell binding.

In this study, pulldown experiments on whole cells indicate that R28$_{Nt}$ binds other integrins, namely $\alpha3\beta1$, $\alpha6\beta1$, and $\alpha6\beta4$ (Fig. 5). Furthermore, we demonstrate by protein–protein binding experiments that the binding is direct. Among already-described GAS direct interactions, Scl1 interacts with integrins $\alpha11\beta1$ and $\alpha2\beta1$ (42, 43), SDH interacts with urokinase plasminogen activator receptor (44), M6 and M1 interacts with CD46 (45, 46), and hyaluronic acid capsule interacts with CD44 (47). The direct binding of GAS to $\alpha3\beta1$, $\alpha6\beta1$, and $\alpha6\beta4$ had never been described thus far. Cervical cells, endometrial epithelial cells, and decidual cells all express, among others, the integrin subunits $\alpha3$, $\alpha6$, $\beta1$ and $\beta4$ (32, 48–50). The R28$_{Nt}$ interaction with integrins $\alpha3\beta1$, $\alpha6\beta1$, and $\alpha6\beta4$ could therefore account for the binding of R28$_{Nt}$ to all these endometritis-related cells (Fig. 2).

The $\alpha3\beta1$, $\alpha6\beta1$, and $\alpha6\beta4$ may not be the sole R28$_{Nt}$ ligands. Indeed, we did not assay the direct interaction of R28$_{Nt}$ with all pulled-down proteins, and the other candidates may interact indirectly, *via* the pulled-down integrins, or directly with R28$_{Nt}$. Other cell surface proteins could also interact with R28$_{Nt}$ and be missed in our screen because our co-immunoprecipitation experiments were carried out with HEC-1A cells; different cell types express different proteins, including different integrins. Further analyses may thus highlight other eukaryotic R28 receptors. Similarly, ACP binds $\alpha1\beta1$ but may also bind other integrins (28) and among them $\alpha3\beta1$, $\alpha6\beta1$, or $\alpha6\beta4$.

Our data suggesting that both R28-N1 and R28-N2 shared a receptor, we tested whether they both interacted directly with the three integrins, which they did (Fig. 5), supporting our com-

petitive assay conclusion. To further characterize the interactions between $R28_{Nt}$ and integrins, we assayed the influence of Mn^{2+} and Ca^{2+} on them. Our data suggested that at the molecular level, the interactions between $R28_{Nt}$ and the various integrins are different and that cations induced conformational changes to $\alpha3\beta1$ and $\alpha6\beta1$, but not of $\alpha6\beta4$, which interferes with $R28_{Nt}$ binding. Most integrin ligands require cations for their interactions, but although not often described, cation-independent interactions of integrins with proteins from pathogens have already been reported, for example between the $\alpha V\beta5$ integrin and the HIV Tat protein (51). Defining the R28 amino acid residues involved in the interaction would provide clues regarding the molecular mechanism taking place. Establishing the structure of R28-N2 would shed light on the sequences potentially interacting with the various receptors and provide a framework for mutational analysis. ACP binds $\alpha1\beta1$ through a KTD sequence located in a β-sandwich subdomain (24, 28). However, R28 harbors no KTD or related sequence and interacts with other integrins; it will be interesting to determine whether the same β-sandwich subdomain is nevertheless involved (Fig. 1*A*).

The absence of significant competition between ACP and R28-N2 could be related to the strong difference of affinity between R28-N2 and ACP for HEC-1-A binding. Also, the absence of competition between R28-N1 and ACP-bound beads could be a consequence of ACP and R28-N1 presenting distinct affinity for some receptors or ACP recognizing additional receptors.

R28 promotes direct binding to the cells. However, this is not the sole binding involved in the adhesion of GAS with hDSC as indicated by the fact that the mutant strain still adheres to the cells. GAS adhesion is a two-step process, a first more labile adhesion involving lipoteichoic acid followed by a second more specific and stronger adhesion involving adhesins (52). Many adhesins have been described, and the interactions with epithelial cell surface receptors have been thoroughly studied (reviewed in Refs. 32, 47, and 48). Most interactions are indirect; proteins of the extracellular matrix, such as fibronectin, form bridges with the host cells. GAS possesses numerous fibronectin-binding proteins, including the M protein that is variable among the *emm* types and may not play always the exact same role. Also, M1 binds directly CD46 (46) and indirectly $\alpha5\beta1$, *via* fibronectin. The dual interaction is required for efficient epithelial cell invasion (46). The interaction between R28 and integrins could potentiate other association(s) mediated by independent adhesins. More experimental support is needed to draw conclusions.

The involvement of R28 in the association between *emm28* and endometritis has been suggested (18), and our data support this suggestion. However, other factors may be involved in this association. They may be adhesins restricted to few genotypes, including *emm28*, such as Mrp28, M28, Enn28, and FCT type 4 pilus proteins (Sfb1 and Cpa) (53), Epf (39), and some RD2, a *emm28*-specific genomic region, encoded surface proteins (13). The unique conjunction of these proteins in *emm28* strains may confer an advantage for binding to the endometrium. RD2 also encodes other proteins of unknown function, as well as a regulator, and they may be involved in diverse colonization or invasion steps of the endometrial or cervical tissue. The adhesion, colonization, and invasion capacities of single or multiple mutant strains should be assessed.

R28 promotes adhesion to female genital tract cells including epithelial cells, and it was suggested that it may contribute to GAS adhesion to different types of epithelial cells (18). We have shown that, indeed, it also promotes adhesion to endometrial epithelial cells and decidual cells but also to pulmonary epithelial cells and to keratinocytes, natural targets for GAS invasive infections (Fig. 6). HaCaT and A549 both express $\alpha3$, $\alpha6$, $\beta4$, and $\beta1$ at their surface (54, 55) and that $R28_{Nt}$ interacts with the different corresponding dimers probably accounts for the increase of binding of $R28_{Nt}$ beads to these cell lines (Fig. 6). TC7 cells also express these integrins, but their localization is mainly basolateral (35); this could explain the lower binding of $R28_{Nt}$ to the apical side of TC7 cells compared with the other cell lines. This ability of $R28_{Nt}$ to promote adhesion to several cell lines, at least partially through integrins, suggests that expressing R28 is an advantage for *emm28* strains that is not limited to endometritis. This may represent a physiological explanation for the fact that *emm28* genotype is a prevalent genotype, being the first to third most encountered *emm* type in invasive infections, in most European countries (9, 10). Other *emm28*-specific virulence factors could also participate in the prevalence and warrant further study. In conclusion, through direct interaction with integrins, R28 supports *emm28* strains elicited endometritis and also contributes to the prevalence of this genotype.

Experimental procedures

Bacterial strains and growth conditions

The strains used in this study are described in Table S1. The M28PF1 strain is a clinical isolate responsible for an endometritis (French National Reference Center for streptococci) that was selected on phenotypic and genotypic bases from a collection of 50 *emm28*-independent clinical isolates (56). GAS strains were grown under static condition at 37 °C in Todd Hewitt medium supplemented with 0.2% yeast extract (THY) or on THY agar plates. *L. lactis* strains were grown in Todd Hewitt medium, supplemented with 10 μg/ml erythromycin when necessary, at 30 °C without agitation or on Todd Hewitt agar plates. *Escherichia coli* strains were cultured in tryptic soy medium at 37 °C with agitation with, when necessary, added antibiotics at the following concentrations: 150 μg/ml erythromycin and 100 μg/ml ticarcillin.

Genetic constructions and generation of the Δ*R28* mutant

The DNA fragments encoding the proteins without signal peptide of $R28_{Nt}$, R28-N1, R28-N2, ACP, and Rib_{Nt+2R} (nt 169–1272, nt 169–688, nt 688–1272, nt 154–681, and nt 171–1188, respectively) were amplified and cloned into pET2818 as described in Ref. 57. All fragments were amplified by PCR using genomic DNA from M28PF1, except for the fragments encoding ACP and Rib_{Nt+2R}, which were amplified from GBS strains A909 and BM110, respectively; the primers used are described in Table S2. The plasmid pOri_$R28_{Nt}$ contains the promoter of *hvgA* deleted of the *covR* consensus boxes, the signal peptide of the GBS BM110 surface protein HvgA, and the LP*X*TG anchor

signal of HvgA subcloned from pAT28-covSP +SPA (57), with the addition of the sequence encoding R28$_{Nt}$ subcloned from pET2818_R28$_{Nt}$. The different plasmids constructed and used during this study are described in Table S1.

The ΔR28 strain corresponds to an in-frame deletion mutant of the gene *Spy1336* encoding the R28 protein and was obtained by homologous recombination of the plasmid pG1-R28 following the same protocol as previously (57). The strain was entirely sequenced as described previously (56). No other significant mutation was found compared with the parent strain M28PF1 except for the gene deletion (56). The primers used for the generation of the plasmid pG1-R28 are described in Table S2. The *L. lactis* strain was transformed by electroporation (58) with the empty vector (CCH2022) or pOri_R28$_{Nt}$ (CCH2023).

Protein production and purification

Peptide expressions were performed with the corresponding derived pET2818 plasmids (Table S1) and purification as described in Ref. 57, except for the gel filtration step, which we did not perform. Peptides purity were confirmed using a 12% SDS–PAGE acrylamide gel and Coomassie Blue staining (Fig. S1*C*).

Antibodies

All animal experiments described in this study were conducted in accordance with guidelines of Paris Descartes University, in compliance with the European animal welfare regulation and were approved by the Institut Cochin University Paris Descartes animal care and use committee (approval 12-145). Mouse anti-R28$_{Nt}$ anti-serum was produced as follows. BalbC 6-week-old mice (Janvier laboratory) were subcutaneously injected with 100 μl of 50 μg/ml R28$_{Nt}$ solution in PBS + aluminum adjuvant. 2 and 4 weeks after the initial injection, the mice were injected with 100 μl of a 25 μg/ml solution. The antibody purity and titer were determined a week after the last injection and assessed by Western blotting experiments. The purified R28-N1 or R28-N2 were injected into rabbits to produce polyclonal antibodies (Covalab). The following antibodies were used throughout the study: anti-α3 integrin (P1B5; DSHB), rabbit anti-α6 integrin (Novus) for ELISA, mouse anti-α6 integrin (P5G10; DSHB) for immunofluorescence, mouse anti-β1 integrin (P5D2; DSHB,) and rat anti-β1 integrin (AIIB2, DSHB).

Bacterial cell wall extracts

Overnight cultures of *L. lactis* were diluted 1/100 in 50 ml of TH broth and cultivated to DO = 0.5. Bacteria were centrifuged 10 min at 5000 rpm at 4 °C, and the pellet was washed once in wash buffer (1× cold PBS, 10 mM EDTA, 1 mM phenylmethylsulfonyl fluoride). The bacteria were centrifuged, and the pellet was resuspended in 250 μl of mutanolysin buffer (20 mM Tris-HCl, pH 7.5, 1 M sucrose, 10 mM EDTA, 1 mM phenylmethylsulfonyl fluoride, 1× protease inhibitor mixture (Roche), 200 units/ml mutanolysin (Sigma)) and incubated for 90 min at 37 °C. The protoplast suspension is then centrifuged for 15 min at 10,000 rpm, and 30 μl of the supernatant containing the cell wall extract is loaded on an acrylamide gel.

Cell culture

HEC-1-A (ATCC® HTB-112™) and ME-180 (ATCC® HTB-33™) cells were cultured as recommended, in McCoy's 5A medium (Gibco) supplemented with 10% fetal bovine serum at 37 °C, 5% CO_2. A549 (ATCC® CCL-185™), HaCaT (Addex-Bio T0020001), and Caco/TC7 cells (CVCL_0233) were cultivated as recommended, in RPMI medium + 10% fetal bovine serum.

Isolation and culture of hDSCs

Decidual stromal cells were isolated from decidua parietalis, obtained from fetal membranes of nonlaboring women after a normal term (>37 weeks of gestation) singleton pregnancy delivered by elective cesarean section. The study of the human fetal membranes was approved by the local ethics committee (Comité de Protection des Personnes Ile de France XI, approval 11018, March 3, 2011), and informed consent was obtained from all donors. Furthermore, the study abides to the Declaration of Helsinki principles. Briefly, fetal membranes were dissected from placenta under sterile conditions, and decidua attached to chorion leaf was peeled off amnion and placed in PBS. After the removal of blood clots, choriodecidua was cut in small pieces and digested with 0.2% collagenase B (Roche Diagnostics) in DMEM-F12 (Invitrogen) at 37 °C for 1.5 h. After the addition of DMEM-F12 containing 5% FCS and 100 μM EDTA, the cell suspension was filtered through 100-μm nylon gauze and centrifuged at 400 × *g* for 10 min. The cell pellet, resuspended in complete medium (DMEM-F12 containing 5% FCS, 100 IU/ml penicillin (Invitrogen), 100 μg/ml streptomycin (Invitrogen)), was plated at a density of 10^5 cells/cm^2 and cultured in complete medium at 37 °C in 5% CO_2 and 95% air in 75-cm^2 flasks overnight. The medium was then renewed after several PBS washes. The cells were harvested with trypsin/EDTA when the cells were 90% confluent. The hDSCs were expanded further to passages 2–4 and thereafter used in the experiments. hDSCs from at least two different women were used.

Adhesion of bacteria to cells

GAS strains M28PF1 (WT) and ΔR28 were diluted from an overnight culture, grown to the exponential phase at an OD = 0.5, and diluted in RPMI medium without glutamine to obtain a multiplicity of infection of 1. Confluent hDSCs in 24-well plates were washed three times, bacterial solution was added, and plates were centrifuged 5 min at 1000 rpm to synchronize bacterial adhesion. After 1 h of incubation at 4 °C, the cells were washed three times with PBS and lysed with distilled water. Serial dilutions of cellular lysates were plated on THYA plates, and the number of CFUs was determined after 24–48 h growth at 37 °C. Six independent experiments were performed in triplicate, and ΔR28 values were normalized to WT adhesion for each independent experiment. Statistical analysis was performed using the one-sample *t* test with GraphPad Prism 5.0.

For adhesion assay of *L. lactis* on HEC-1-A, the cells were seeded 72 h prior to infection to reach confluence at 5–10 × 10^6 cells/well in 24-well plates. The protocols for the *L. lactis* CCH2022 and CCH2023 bacterial preparation and adhesion to cells was the same as above. For all experiments, three indepen-

dent assays in triplicate were carried out for each infection. Paired *t* tests were performed with GraphPad Prism 5.0.

ELISA-based protein–cell interaction assay

The cell–protein binding assay protocol derives from Bolduc and Madoff (28). Briefly, the cells are incubated with biotinylated proteins in PBS with 1% BSA for 1 h at 4 °C and then washed, and bound proteins are revealed by streptavidin–HRP (GE Healthcare) and subsequent *O*-phenyldiamine (Sigma) revelation. Number of moles of biotin per mole of protein was evaluated using an HABA kit (Life Technologies): the ratio of biotin molecule per peptide molecule was ~5, except for Rib_{Nt+2R}, for which it reached 9. Therefore, the fluorescence values obtained for Rib_{Nt+2R} were divided by 2 for comparison sake. Experiments were performed four times independently, except for Rib_{Nt+2R} performed three times. Statistical analysis was performed after nonlinear fitting using a second order polynomial quadratic model and comparison of the extra sum of squares F-test of the best fit values using GraphPad Prism 5.0. The curves were fitted with an equation: Absorbance = B1 * concentration + B2* (concentration)^2. Because this equation did not fit the BSA curve, statistical analysis to BSA were performed with two-way ANOVA with Bonferroni post-tests at maximum binding.

Bead fixation to cells

Fluosphere (Invitrogen, yellow green, 1 μm) were coupled with the different peptides following the manufacturer's recommendations. Correct coupling was confirmed by cytometric analysis with appropriate antisera. Indicated confluent cells in dark 96-well plates (Nunc, Life Technologies) were washed three times with cold PBS supplemented with 1 mM Ca^{2+} and 1 mM Mg^{2+} (PBS++). The beads were diluted to a concentration of 10^8 beads/ml in cold PBS++, and 150 μl of beads solution was added to cells and incubated 1 h at 4 °C. The cells were washed three times in PBS++, fixed 15 min at room temperature in paraformaldehyde 1%, and quenched with 50 mM NH_4Cl. Fluorescence of the inoculum solutions, cells, and cells incubated with beads was measured with a TECAN fluorescent plate reader with a GFP filter. Fluorescence of adherent beads corresponds to the fluorescence of the total well subtracted by the autofluoresence of a well containing cells only.

For competition assays, prior to beads adhesion, the cells were incubated with 20 μM of specified peptide in PBS++ for 1 h at 4 °C; the beads were then added, and the experiments performed as described above. For antibody competition, the beads were incubated with 10 μg/ml of purified anti-R28-N1 and anti-R28-N2 rabbit antibodies for 1 h at 4 °C prior to incubation with cells. The experiments were performed at least three times in duplicate. Statistical analyses were performed with two-way ANOVA.

Flow cytometry analysis of protein binding to eukaryotic cells after different treatments

Confluent 72 h HEC-1-A cells were dissociated with cell dissociation buffer (Life Technologies) and treated with $NaIO_4$ (Sigma), Pronase (Life Technologies), trypsin (Worthington Biochemical Corporation), phospholipase A_2 (Sigma), or heparinase I (NEB) at the specified concentrations and as described by Gallotta *et al.* (33). The cells were then incubated with 20 μM soluble $R28_{Nt}$, R28-N1, or R28-N2 in PBS with 0.5% BSA and stained with mouse antiserum and secondary anti-mouse PE coupled antibody. Fluorescence of cells was measured in an Accuri C6 BD cytometer. 100% staining was considered with cells untreated (control). Unspecific labeling of cells by mouse antiserum and secondary antibodies was measured on untreated cells that were not incubated with the peptides but underwent the same labeling protocol (without peptide condition). Experiments were performed at least three times independently. Two-way ANOVA analysis was performed with GraphPad Prism 5.

Protein sequence comparison

These comparisons were carried out using the BlastP algorithm (https://blast.ncbi.nlm.nih.gov/Blast.cgi?PAGE=Proteins&PROGRAM=blastp&BLAST_PROGRAMS=blastp&PAGE_TYPE=BlastSearch&BLAST_SPEC=blast2seq&DATABASE=n/a&QUERY=&SUBJECTS=).[5]

In silico protein structure prediction

Peptide structure was made using Phyre software (http://www.sbg.bio.ic.ac.uk/phyre2/html/page.cgi?id=index).[5]

Co-immunoprecipitation of cross-linked $R28_{Nt}$ receptors

HEC-1-A cells grown to confluence in T25 flask were washed three times with cold PBS++. A 6-ml solution of cold PBS++, 1% BSA, with or without (control) 20 μM $R28_{Nt}$ was added, and incubation was pursued for 1 h on ice. The cells were washed three times in cold PBS++ and 10 ml of 1 mM DTSSP (Thermo Fisher) was added for 2 h on ice. After one wash with PBS++, cross-linking was blocked with 10 ml of 50 mM Tris, pH 7.5, for 10 min on ice. An equimolar mix of rabbit polyclonal anti–R28-N1 and –R28-N2 antibodies (1 mg/ml total, 1.7 ml per flask) was added to two freshly washed HEC-1-A T25 flask for 10 min to adsorb unspecific cell binding antibodies. Preadsorbed antibodies (1.5 ml) were added to each flask and incubated for 1 h at 4 °C. Unbound antibodies were removed by three washes with PBS++, and the cells were lysed for 1 h at 4 °C with 1.5 ml of lysis buffer (PBS, 1× protease inhibitor mixture (Thermo Fisher), phenylmethylsulfonyl fluoride 1 mM (Sigma), and 1% SurfactAmp Triton X-100 (Thermo Fisher)). Lysates were centrifuged at 15,000 × *g* for 15 min at 4 °C, and supernatants were incubated with 100 μl magnetic protein A beads (Pierce) for 1 h at 20 °C. Beads were then washed six times with 1.5 ml of PBS, 500 mM NaCl, and 1% Triton, and complexes were eluted in Laemmli buffer in disulfide-bond preservation conditions (60 mM Tris, pH 6.8, 1% SDS) at 95 °C for 5 min. The gels were run in duplicate; one gel was used for Western blotting with 15% of the eluates, revealed with mouse anti-$R28_{Nt}$ antiserum to reveal cross-linked complexes, and the other gel was used for their identification by MS. The Western blotting indicated that $R28_{Nt}$ complexes were found above 170 kDa.

[5] Please note that the JBC is not responsible for the long-term archiving and maintenance of this site or any other third party hosted site.

Short migration SDS–PAGE, protein trapping, and peptide extraction

85% of the eluate was loaded in the same condition as above for a 2-cm migration and then stained with colloidal Coomassie Blue (Quick Coomassie stain from Clinisciences). Stained gels allowed visualization of protein abundance and molecular mass distribution. Protein-containing gel lanes from the two conditions (with the bait R28 and in its absence, control condition) were excised above the 170-kDa molecular mass marker (Life Technologies Pageruler prestained protein ladder). The polyacrylamide gel constitutes a matrix where successive protein treatments were performed: salt, buffer, and detergent removal by successive washes of 100 mM NH_4HCO_3 (or ABC) and 50% acetonitrile; disulfide-bond removal by cysteine reduction in ABC + 10 mM DTT at 56 °C for 30 min; free thiol protection by alkylation in ABC + 55 mM chloroacetamide for 30 min at room temperature; and overnight digestion with trypsin. Peptides were then extracted using washes of 5% formic acid intercalated with gel shrinkages in 50% acetonitrile. All washes were pooled and evaporated before analysis.

C18 liquid nanochromatography and MS

Mass spectrometry analyses were performed at the 3P5 proteomics facility of the University Paris Descartes using an U3000 RSLC nano-LC system hyphenated to an Orbitrap fusion mass spectrometer (all from Thermo Fisher Scientific). Peptides were solubilized in 7 μl of 0.1% TFA containing 10% acetonitrile. They were loaded, concentrated, and washed for 3 min on a C18 reverse-phase precolumn (3-μm particle size, 100 Å pore size, 75-μm inner diameter, 2-cm length; Thermo Fischer Scientific). Peptides were separated on a C18 reverse-phase resin (2-μm particle size, 100 Å pore size, 75-μm inner diameter, 25-cm length; Thermo Fisher Scientific) with a 35-min binary gradient starting from 99% of solvent A containing 0.1% formic acid in H_2O and ending in 40% of solvent B containing 80% acetonitrile, 0.085% formic acid in H_2O. The mass spectrometer acquired data throughout the elution process and operated in a data-dependent scheme with full MS scans acquired with the Orbitrap, followed by as many MS/MS ion trap CID spectra 5 s can fit (data-dependent acquisition with top speed mode: 5-s cycle) using the following settings: full MS automatic gain control: $2.10e^5$, maximum ion injection time: 60 ms, resolution: $6.10e^4$, m/z range 350–1500 and for MS/MS; isolation width: 1.6 Th, minimum signal threshold: 5000, automatic gain control $2.10e^4$, maximum ion injection time: 100 ms, peptides with undefined charge state or charge state of 1 were excluded from fragmentation, dynamic exclusion time: 30 s.

Identifications (protein hits) and quantifications were performed by comparison of experimental peak lists with a database of theoretical sequences using MaxQuant version 1.6.1.0 (59). The databases used were the human sequences from the curated Uniprot database (release June 2018) and a list of in-house contaminant sequences. Carbamidomethylation of cysteines was set as constant modification, whereas acetylation of the protein N terminus and oxidation of methionines were set as variable modifications. The false discovery rate was kept below 1% on both peptides and proteins. The "match between runs" option was not allowed. For analysis, results from MaxQuant were imported into the Perseus software version 1.6.1.1 (60). Reverse and contaminant proteins (human keratins and nonhuman proteins) were excluded from analysis. Proteins of interest were selected based on reported intensity in three of three replicates for each group. All hits are presented in the supporting data file.

Selection of positive hits

The enrichment is defined as the ratio of raw intensity of the co-immunoprecipitation identified proteins in the $R28_{Nt}$ bait conditions compared with the control condition. Hits with a ratio above 1 and/or no peptide found in the control condition for all three independent experiments performed were considered as specifically enriched in the presence of R28. From this list, only surface-exposed proteins are shown in Table 1.

Immunolabeling of bound $R28_{Nt}$ and coated fluospheres on HEC-1-A

72 h after seeding on glass coverslips in 24-well plates, confluent HEC-1-A cells were washed three times in cold PBS++. A 10 μM solution of $R28_{Nt}$ in PBS++, 1% BSA was added to the cells for 1 h at 4 °C. The cells were washed three times in cold PBS++ and fixed 15 min at 20 °C with 1% paraformaldehyde. The cells were quenched with 50 mM ammonium chloride and blocked for 30 min with PBS, 3% BSA. The cells were incubated with primary antibodies for 1 h at 20 °C in PBS, 1% BSA. The cells were washed and incubated with secondary antibodies and DAPI at 1/5 000 for 1 h at 20 °C. The coverslips were mounted on slides with Mowiol and imaged on a Leica DMI6000, and the images were analyzed with ImageJ.

For the observation of bound coated fluospheres, 10^8 coated beads in PBS++ were added to the cells and treated as above. The Beads did not require labeling because they are intrinsically fluorescent.

ELISA

To evaluate integrin binding to immobilized $R28_{Nt}$ or its subdomains R28-N1 and R28-N2, ELISAs were performed essentially as described by Six *et al.* (57). Proteins were coated at 5 μg/ml overnight. 50 μl of integrins (human recombinant extracellular domain, tested for their ability to interact with known ligands; R&D) were incubated 2 h at 37 °C at the specified concentrations diluted in PBS, 1% BSA. Rat anti-β1 (AIIB2, DSHB) and rabbit anti-α6 (R&D) antibodies were used at a 1/200 dilution. Experiments were performed at least three times. The statistical analyses were performed as described above for the ELISA based protein–cell interaction assay.

The importance of divalent cations for the interaction between $R28_{Nt}$ and integrins was tested by ELISA with the same coating protocol as above with 50 μl at 10 μg/ml of integrins added to the wells. All solutions for the assay were made in PBS, PBS + 10 mM EDTA, PBS + 1 mM Mn^{2+}, and PBS + 1 mM Ca^{2+}, as specified. Detection and revelation were performed as above. The values were normalized on the binding to the integrins in the presence of EDTA. One-way ANOVA was performed to compare the four independent experiments.

Author contributions—A. W., C. Poyart, and A. F. conceptualization; A. W. data curation; A. W. and A. F. formal analysis; A. W. validation; A. W., D. A., S. B., C. M., C. Plainvert, M. L., and A. F. investigation; A. W., S. B., C. M., and A. F. methodology; A. W. and A. F. writing-original draft; A. W., C. Poyart, and A. F. writing-review and editing; C. M., C. Poyart, and A. F. funding acquisition; C. Poyart and A. F. project administration; A. F. supervision.

Acknowledgments—We thank Wassim El Nemer, Julie Guignot, and Cecile Arrieumerlou for helpful discussions and Philippe Glaser for sequencing and providing the relevant contigs of the ΔR28 strain. We thank Cédric Broussard (LC–MS supervision and in-gel protein digestion); Evangeline Bennana (proteomics data collection, analysis, and reporting), Marjorie Leduc (LIMS management); and François Guillonneau, Philippe Chafey, and Patrick Mayeux (proteomics expertise and experimental design) from the 3P5 proteomics facility of the Université Paris Descartes, Sorbonne Paris Cité and the Imag'IC facility, both at the Cochin Institute. We thank the Margottin–Pique team for access to the TECAN plate reader. The Orbitrap Fusion mass spectrometer was acquired with funds from the European Regional Development Fund (ERDF) through the Operational Programme for Competitiveness Factors and Employment 2007–2013 and from the Canceropole Ile de France.

References

1. Bisno, A. L., Brito, M. O., and Collins, C. M. (2003) Molecular basis of group A streptococcal virulence. *Lancet Infect. Dis.* **3,** 191–200 CrossRef Medline
2. Tart, A. H., Walker, M. J., and Musser, J. M. (2007) New understanding of the group A *Streptococcus* pathogenesis cycle. *Trends Microbiol.* **15,** 318–325 CrossRef Medline
3. Cunningham, M. W. (2000) Pathogenesis of group A streptococcal infections. *Clin. Microbiol. Rev.* **13,** 470–511 CrossRef Medline
4. Carapetis, J. R., Steer, A. C., Mulholland, E. K., and Weber, M. (2005) The global burden of group A streptococcal diseases. *Lancet Infect. Dis.* **5,** 685–694 CrossRef Medline
5. Beall, B., Facklam, R., and Thompson, T. (1996) Sequencing emm-specific polymerase chain reaction products for routine and accurate typing of group A streptococci. *J. Clin. Microbiol.* **34,** 953–958 Medline
6. Li, Z., Sakota, V., Jackson, D., Franklin, A. R., Beall, B., and the Active Bacterial Core Surveillance/Emerging Infections Program Network (2003) Array of M protein gene subtypes in 1064 recent invasive group A streptococcus isolates recovered from the active bacterial core surveillance. *J. Infect. Dis.* **188,** 1587–1592 CrossRef Medline
7. Bessen, D. E. (2016) Tissue tropisms in group A *Streptococcus*: what virulence factors distinguish pharyngitis from impetigo strains? *Curr. Opin. Infect. Dis.* **29,** 295–303 CrossRef Medline
8. Beres, S. B., and Musser, J. M. (2007) Contribution of exogenous genetic elements to the group A *Streptococcus metagenome*. *PLoS One* CrossRef
9. Gherardi, G., Vitali, L. A., and Creti, R. (2018) Prevalent emm types among invasive GAS in Europe and North America since year 2000. *Front. Public Health* **6,** 59 CrossRef Medline
10. Plainvert, C., Doloy, A., Loubinoux, J., Lepoutre, A., Collobert, G., Touak, G., Trieu-Cuot, P., Bouvet, A., Poyart, C., and CNR-Strep Network (2012) Invasive group A streptococcal infections in adults, France (2006–2010). *Clin. Microbiol. Infect.* **18,** 702–710 CrossRef Medline
11. Green, N. M., Beres, S. B., Graviss, E. A., Allison, J. E., McGeer, A. J., Vuopio-Varkila, J., LeFebvre, R. B., and Musser, J. M. (2005) Genetic diversity among type emm28 group A *Streptococcus* strains causing invasive infections and pharyngitis. *J. Clin. Microbiol.* **43,** 4083–4091 CrossRef Medline
12. Colman, G., Tanna, A., Efstratiou, A., and Gaworzewska, E. T. (1993) The serotypes of *Streptococcus pyogenes* present in Britain during 1980–1990 and their association with disease. *J. Med. Microbiol.* **39,** 165–178 CrossRef Medline
13. Green, N. M., Zhang, S., Porcella, S. F., Nagiec, M. J., Barbian, K. D., Beres, S. B., LeFebvre, R. B., and Musser, J. M. (2005) Genome sequence of a serotype M28 strain of group a *Streptococcus*: potential new insights into puerperal sepsis and bacterial disease specificity. *J. Infect. Dis.* **192,** 760–770 CrossRef Medline
14. Sitkiewicz, I., Green, N. M., Guo, N., Mereghetti, L., and Musser, J. M. (2011) Lateral gene transfer of streptococcal ICE element RD2 (region of difference 2) encoding secreted proteins. *BMC Microbiol.* **11,** 65 CrossRef Medline
15. Baker, C. J., Goroff, D. K., Alpert, S., Crockett, V. A., Zinner, S. H., Evrard, J. R., Rosner, B., and McCormack, W. M. (1977) Vaginal colonization with group B *Streptococcus*: a study in college women. *J. Infect. Dis.* **135,** 392–397 CrossRef Medline
16. Nobbs, A. H., Lamont, R. J., and Jenkinson, H. F. (2009) *Streptococcus* adherence and colonization. *Microbiol. Mol. Biol. Rev.* **73,** 407–450 CrossRef Medline
17. Courtney, H. S., Hasty, D. L., and Dale, J. B. (2002) Molecular mechanisms of adhesion, colonization, and invasion of group A streptococci. *Ann. Med.* **34,** 77–87 CrossRef Medline
18. Stålhammar-Carlemalm, M., Areschoug, T., Larsson, C., and Lindahl, G. (1999) The R28 protein of *Streptococcus pyogenes* is related to several group B streptococcal surface proteins, confers protective immunity and promotes binding to human epithelial cells. *Mol. Microbiol.* **33,** 208–219 CrossRef Medline
19. Wästfelt, M., Stålhammar-Carlemalm, M., Delisse, A. M., Cabezon, T., and Lindahl, G. (1996) Identification of a family of streptococcal surface proteins with extremely repetitive structure. *J. Biol. Chem.* **271,** 18892–18897 CrossRef Medline
20. Lachenauer, C. S., Creti, R., Michel, J. L., and Madoff, L. C. (2000) Mosaicism in the α-like protein genes of group B streptococci. *Proc. Natl. Acad. Sci. U.S.A.* **97,** 9630–9635 CrossRef Medline
21. Lindahl, G., Stålhammer-Carlemalm, M., and Areschoug, T. (2005) Surface proteins of *Streptococcus agalactiae* and related proteins in other bacterial pathogens. *Clin. Microbiol. Rev.* **18,** 102–127 CrossRef Medline
22. Callebaut, I., Gilgès, D., Vigon, I., and Mornon, J. P. (2000) HYR, an extracellular module involved in cellular adhesion and related to the immunoglobulin-like fold. *Protein Sci.* **9,** 1382–1390 CrossRef Medline
23. Glaser, P., Rusniok, C., Buchrieser, C., Chevalier, F., Frangeul, L., Msadek, T., Zouine, M., Couvé, E., Lalioui, L., Poyart, C., Trieu-Cuot, P., and Kunst, F. (2002) Genome sequence of *Streptococcus agalactiae*, a pathogen causing invasive neonatal disease. *Mol. Microbiol.* **45,** 1499–1513 CrossRef Medline
24. Aupérin, T. C., Bolduc, G. R., Baron, M. J., Heroux, A., Filman, D. J., Madoff, L. C., and Hogle, J. M. (2005) Crystal structure of the N-terminal domain of the group B *Streptococcus* αC protein. *J. Biol. Chem.* **280,** 18245–18252 CrossRef Medline
25. Stålhammar-Carlemalm, M., Areschoug, T., Larsson, C., and Lindahl, G. (2000) Cross-protection between group A and group B streptococci due to cross-reacting surface proteins. *J. Infect. Dis.* **182,** 142–149 CrossRef Medline
26. Baron, M. J., Bolduc, G. R., Goldberg, M. B., Aupérin, T. C., and Madoff, L. C. (2004) αC protein of group B *Streptococcus* binds host cell surface glycosaminoglycan and enters cells by an actin-dependent mechanism. *J. Biol. Chem.* **279,** 24714–24723 CrossRef Medline
27. Baron, M. J., Filman, D. J., Prophete, G. A., Hogle, J. M., and Madoff, L. C. (2007) Identification of a glycosaminoglycan binding region of the αC protein that mediates entry of group B streptococci into host cells. *J. Biol. Chem.* **282,** 10526–10536 CrossRef Medline
28. Bolduc, G. R., and Madoff, L. C. (2007) The group B streptococcal αC protein binds α1β1-integrin through a novel KTD motif that promotes internalization of GBS within human epithelial cells. *Microbiology* **153,** 4039–4049 CrossRef Medline
29. Bolduc, G. R., Baron, M. J., Gravekamp, C., Lachenauer, C. S., and Madoff, L. C. (2002) The αC protein mediates internalization of group B *Streptococcus* within human cervical epithelial cells. *Cell Microbiol.* **4,** 751–758 CrossRef Medline

30. Chapot-Chartier, M. P., Vinogradov, E., Sadovskaya, I., Andre, G., Mistou, M. Y., Trieu-Cuot, P., Furlan, S., Bidnenko, E., Courtin, P., Péchoux, C., Hols, P., Dufrêne, Y. F., and Kulakauskas, S. (2010) Cell surface of *Lactococcus lactis* is covered by a protective polysaccharide pellicle. *J. Biol. Chem.* **285,** 10464–10471 CrossRef Medline
31. Areschoug, T., Carlsson, F., Stålhammar-Carlemalm, M., and Lindahl, G. (2004) Host-pathogen interactions in *Streptococcus pyogenes* infections, with special reference to puerperal fever and a comment on vaccine development. *Vaccine.* **22,** S9–S14 CrossRef Medline
32. Castelbaum, A. J., Ying, L., Somkuti, S. G., Sun, J., Ilesanmi, A. O., and Lessey, B. A. (1997) Characterization of integrin expression in a well differentiated endometrial adenocarcinoma cell line (Ishikawa). *J. Clin. Endocrinol. Metab.* **82,** 136–142 CrossRef Medline
33. Gallotta, M., Gancitano, G., Pietrocola, G., Mora, M., Pezzicoli, A., Tuscano, G., Chiarot, E., Nardi-Dei, V., Taddei, A. R., Rindi, S., Speziale, P., Soriani, M., Grandi, G., Margarit, I., and Bensi, G. (2014) SpyAD, a moonlighting protein of group A *Streptococcus* contributing to bacterial division and host cell adhesion. *Infect. Immun.* **82,** 2890–2901 CrossRef Medline
34. Luca-Harari, B., Darenberg, J., Neal, S., Siljander, T., Strakova, L., Tanna, A., Creti, R., Ekelund, K., Koliou, M., Tassios, P. T., van der Linden, M., Straut, M., Vuopio-Varkila, J., Bouvet, A., Efstratiou, A., *et al.* (2009) Clinical and microbiological characteristics of severe *Streptococcus pyogenes* disease in Europe. *J. Clin. Microbiol.* **47,** 1155–1165 CrossRef Medline
35. Hamzaoui, N., Kernéis, S., Caliot, E., and Pringault, E. (2004) Expression and distribution of β1 integrins in *in vitro*-induced M cells: implications for *Yersinia* adhesion to Peyer's patch epithelium. *Cell Microbiol.* **6,** 817–828 CrossRef Medline
36. Nobbs, A. H., Jenkinson, H. F., and Everett, D. B. (2015) Generic determinants of *Streptococcus* colonization and infection. *Infect. Genet. Evol.* **33,** 361–370 CrossRef Medline
37. Brouwer, S., Barnett, T. C., Rivera-Hernandez, T., Rohde, M., and Walker, M. J. (2016) *Streptococcus pyogenes* adhesion and colonization. *FEBS Lett.* **590,** 3739–3757 CrossRef Medline
38. Rohde, M., and Cleary, P. P. (2016) Adhesion and invasion of *Streptococcus pyogenes* into host cells and clinical relevance of intracellular streptococci. In *Streptococcus pyogenes: Basic Biology to Clinical Manifestations*, pp. 1–39, University of Oklahoma, Norman, OK
39. Linke, C., Siemens, N., Oehmcke, S., Radjainia, M., Law, R. H., Whisstock, J. C., Baker, E. N., and Kreikemeyer, B. (2012) The extracellular protein factor epf from *Streptococcus pyogenes* is a cell surface adhesin that binds to cells through an N-terminal domain containing a carbohydrate-binding module. *J. Biol. Chem.* **287,** 38178–38189 CrossRef Medline
40. Lynskey, N. N., Reglinski, M., Calay, D., Siggins, M. K., Mason, J. C., Botto, M., and Sriskandan, S. (2017) Multi-functional mechanisms of immune evasion by the streptococcal complement inhibitor C5a peptidase. *PLoS Pathog.* **13,** e1006493 CrossRef Medline
41. Kong, F., Gowan, S., Martin, D., James, G., and Gilbert, G. L. (2002) Molecular profiles of group B streptococcal surface protein antigen genes: relationship to molecular serotypes. *J. Clin. Microbiol.* **40,** 620–626 CrossRef Medline
42. Humtsoe, J. O., Kim, J. K., Xu, Y., Keene, D. R., Höök, M., Lukomski, S., and Wary, K. K. (2005) A streptococcal collagen-like protein interacts with the $\alpha 2\beta 1$ integrin and induces intracellular signaling. *J. Biol. Chem.* **280,** 13848–13857 CrossRef Medline
43. Caswell, C. C., Barczyk, M., Keene, D. R., Lukomska, E., Gullberg, D. E., and Lukomski, S. (2008) Identification of the first prokaryotic collagen sequence motif that mediates binding to human collagen receptors, integrins $\alpha 2\beta 1$ and $\alpha 11\beta 1$. *J. Biol. Chem.* **283,** 36168–36175 CrossRef Medline
44. Jin, H., Song, Y. P., Boel, G., Kochar, J., and Pancholi, V. (2005) Group A streptococcal surface GAPDH, SDH, recognizes uPAR/CD87 as its receptor on the human pharyngeal cell and mediates bacterial adherence to host cells. *J. Mol. Biol.* **350,** 27–41 CrossRef Medline
45. Okada, N., Liszewski, M. K., Atkinson, J. P., and Caparon, M. (1995) Membrane cofactor protein (CD46) is a keratinocyte receptor for the M protein of the group A *Streptococcus*. *Proc. Natl. Acad. Sci. U.S.A.* **92,** 2489–2493 CrossRef Medline
46. Rezcallah, M. S., Hodges, K., Gill, D. B., Atkinson, J. P., Wang, B., and Cleary, P. P. (2005) Engagement of CD46 and $\alpha 5\beta 1$ integrin by group A streptococci is required for efficient invasion of epithelial cells. *Cell Microbiol.* **7,** 645–653 CrossRef Medline
47. Cywes, C., Stamenkovic, I., and Wessels, M. R. (2000) CD44 as a receptor for colonization of the pharynx by group A *Streptococcus*. *J. Clin. Invest.* **106,** 995–1002 CrossRef Medline
48. Werner, J., Decarlo, C. A., Escott, N., Zehbe, I., and Ulanova, M. (2012) Expression of integrins and Toll-like receptors in cervical cancer: effect of infectious agents. *Innate Immun.* **18,** 55–69 CrossRef Medline
49. Lessey, B. A., Castelbaum, A. J., Buck, C. A., Lei, Y., Yowell, C. W., and Sun, J. (1994) Further characterization of endometrial integrins during the menstrual cycle and in pregnancy. *Fertil. Steril.* **62,** 497–506 CrossRef Medline
50. Wadehra, M., Forbes, A., Pushkarna, N., Goodglick, L., Gordon, L. K., Williams, C. J., and Braun, J. (2005) Epithelial membrane protein-2 regulates surface expression of $\alpha v\beta 3$ integrin in the endometrium. *Dev. Biol.* **287,** 336–345 CrossRef Medline
51. Vogel, B. E., Lee, S.-J., Hildebrand, A., Craig, W., Pierschbacher, M. D., Wong-Staal, F., and Ruoslahti, E. (1993) A novel integrin specifically exemplified by binding $\alpha v\beta 5$ integrin to the basic domain of the HIV tat protein anmd vitronectin. *J. Cell Biol.* **121,** 461–468 CrossRef Medline
52. Hasty, D. L., Ofek, I., Courtney, H. S., and Doyle, R. J. (1992) Multiple adhesins of streptococci. *Infect. Immun.* **60,** 2147–2152 Medline
53. Köller, T., Manetti, A. G., Kreikemeyer, B., Lembke, C., Margarit, I., Grandi, G., and Podbielski, A. (2010) Typing of the pilus-protein-encoding FCT region and biofilm formation as novel parameters in epidemiological investigations of *Streptococcus pyogenes* isolates from various infection sites. *J. Med. Microbiol.* **59,** 442–452 CrossRef Medline
54. Abban, C. Y., and Meneses, P. I. (2010) Usage of heparan sulfate, integrins, and FAK in HPV16 infection. *Virology* **403,** 1–16 CrossRef Medline
55. Falcioni, R., Cimino, L., Gentileschi, M. P., D'Agnano, I., Zupi, G., Kennel, S. J., and Sacchi, A. (1994) Expression of $\beta 1$, $\beta 3$, $\beta 4$, and $\beta 5$ integrins by human lung carcinoma cells of different histotypes. *Exp. Cell Res.* **210,** 113–122 CrossRef Medline
56. Longo, M., De Jode, M., Plainvert, C., Weckel, A., Hua, A., Château, A., Glaser, P., Poyart, C., and Fouet, A. (2015) Complete genome sequence of *Streptococcus pyogenes* emm28 strain M28PF1, responsible of a puerperal fever. *Genome Announc.* **3,** e00750-15 Medline
57. Six, A., Bellais, S., Bouaboud, A., Fouet, A., Gabriel, C., Tazi, A., Dramsi, S., Trieu-Cuot, P., and Poyart, C. (2015) Srr2, a multifaceted adhesin expressed by ST-17 hypervirulent group B *Streptococcus* involved in binding to both fibrinogen and plasminogen. *Mol. Microbiol.* **97,** 1209–1222 CrossRef Medline
58. Caparon, M. G., and Scott, J. R. (1991) Genetic manipulation of pathogenic Streptococci. *Methods Enzymol.* **204,** 556–586 CrossRef Medline
59. Cox, J., Hein, M. Y., Luber, C. A., Paron, I., Nagaraj, N., and Mann, M. (2014) Accurate proteome-wide label-free quantification by delayed normalization and maximal peptide ratio extraction, termed MaxLFQ. *Mol. Cell Proteomics* **13,** 2513–2526 CrossRef Medline
60. Tyanova, S., Temu, T., Sinitcyn, P., Carlson, A., Hein, M. Y., Geiger, T., Mann, M., and Cox, J. (2016) The Perseus computational platform for comprehensive analysis of (prote)omics data. *Nat. Methods* **13,** 731–740 CrossRef Medline